

# Surface Structure Build-Up and Three-Dimensional Topography of Polyurethane Powder Coatings

Barbara Pilch-Pitera,<sup>1</sup> Ryszard Stagraczyński<sup>2</sup>

<sup>1</sup>Department of Polymer Science, Faculty of Chemistry, Rzeszów University of Technology, Rzeszów 35-959, Poland

<sup>2</sup>Department of Physics, Faculty of Mathematics and Applied Physics, Rzeszów University of Technology, Rzeszów 35-959, Poland

Received 2 February 2010; accepted 3 May 2010

DOI 10.1002/app.32733

Published online 14 July 2010 in Wiley InterScience (www.interscience.wiley.com).

**ABSTRACT:** Non- and polysilsesquioxane-containing polyurethane-based powder coating systems, crosslinked with allophanate bonds containing polyisocyanates were examined. The surface structure built-up of the powder coatings were investigated at different temperatures with a polarized optical microscopy (POM) using reflected light. The three-dimensional surface topography and the values of surface roughness were determined. The surface structure was correlated with the chemical structure of the coat-

ings and macroscopic surface behavior: surface free energy and gloss. These experimental results lead to a better understanding of the development of surface topography and morphology and provide valuable information for the development of new polyurethane powder coating systems. © 2010 Wiley Periodicals, Inc. *J Appl Polym Sci* 118: 3586–3593, 2010

**Key words:** polyurethanes; coatings; surfaces; microstructure

## INTRODUCTION

Polyurethane powder coatings are currently the fastest growing section of powder paints, because of their favorable application attributes and performance advantages. Advances in the formulation of raw materials and process technology enabled their growth into a wide range of applications, most of which require a good corrosion protection, low friction, easy-clean, nonwetting, improved abrasion, thermal, chemical and fire resistance, and good surface appearance. The possibility of gaining improved performance by combining the properties of organic and inorganic components additionally widen a range of their applications.

The research and development in this field covered modern systems into which inorganic components included, like polysilsesquioxanes, polysilanes, polysiloxanes, phosphazenes, inorganic nanofillers (nanosilica, Fe<sub>2</sub>O<sub>3</sub> and TiO<sub>2</sub> nanopowders, talc, mica, montmorillonite, hectorite, laponite, saponite), as well as organic modifiers, e.g. organophosphorus compounds, organo-boranes, fluoropolymers, and polymer nanopowders.<sup>1–5</sup>

In general, surface appearance is described by such parameters as gloss, haze, smooth, rough, wavy, clear, transparency, and color of the surface. These effects are strongly influenced by surface topography and

chemical structure. Surface topography plays an important role in controlling the interaction between materials and the environment. To build the basis for a better understanding of the built-up of the surface appearance, this study focuses on the relationships between the surface chemical structure and the surface properties, such as gloss, roughness, wettability, and surface free energy.<sup>6–9</sup>

In this article, the surface structure built-up during curing and surface topography of the non- and polysilsesquioxane-containing polyurethane powder coatings were investigated and compared. This elaboration makes reference to the published results of our earlier research which covered the synthesis methods, chemical structures, and distribution of molecular weights of blocked polyisocyanates which contained allophanate bonds, and which were used this time as crosslinking agents.<sup>10,11</sup> Our earlier articles presented also the methods for preparing coating formulations and for hardening said coatings, and also the effect of the chemical structures on selected application properties of lacquer coatings.

This article is intended to show the effects of a number of structural parameters and process factors, like chemical structures of polyisocyanate and polyester resins, presence of polysilsesquioxane, as well as lacquer hardening temperature and time, on morphology of supermolecular structures, surface microtopography, gloss, wetting angle, and surface free energy. Also, an attempt was made here to provide some generalization in this field. Moreover, special attention was paid to visualization of the coating hardening process.

Correspondence to: B. Pilch-Pitera (barbpi@prz.edu.pl).

Polarized optical microscopy (POM) with the sample heat-up unit was employed in visualization of the coating formation process and in assessing morphology of obtained coatings. The goal of our research was to observe the blend melting process, polyisocyanate deblocking process, hardening process, and coat formation process, and also to visualize the supermolecular structures formed, and to evaluate the time needed for deblocking and crosslinking. Confocal laser scanning microscopy (CLSM), as well as measurements of the contact angle with various liquids (diiodomethane, formamide, and water) and gloss (for the angles of 20°, 60°, and 85°) were used to characterize the powder coatings and correlating their structure with the macroscopic surface behavior (wettability and gloss characteristics). Based on the obtained results, the effect was discussed of the chemical composition of the lacquer formulations on the superficial structures and properties of so produced coatings.

## EXPERIMENTAL

### Raw materials and reagents

Isophorone diisocyanate (IPDI) – Desmodur I, and 4,4'-dicyclohexylmethane diisocyanate (H<sub>12</sub>MDI) – Desmodur W, from Bayer A.G. (Leverkusen, Germany). Methanol (ME), ethanol (ET), 2-propanol (PR), 1-butanol (BU), and 1-hexanol (HE), from Aldrich (Buchs, Switzerland). 3,5-Dimethylpirazole (DMP), from Aldrich (Buchs, Switzerland). Rucote 102 – polyester resin based on isophthalic acid and neopentyl glycol, acid value: 11–14 mg KOH/g, hydroxyl value: 35–45 mg KOH/g, T<sub>g</sub>: 59°C (RU102), from Bayer A.G. (Leverkusen, Germany). WorleeAdd 902, and Resiflow PV 88, from Worlee – Chemie G.m.b.H (Lauenburg, Germany). Octa(3-aminopropyl)octasilsesquioxane (POSS) (Fig. 1), molecular weight: 880 g/mol, length of the diagonal in elementary cell: 1–3 nm, was synthesized according to the method described in literature by Maciejewski H. et al.<sup>12</sup>

### Synthesis of curing agents for powder lacquers

Allophanate structure containing polyisocyanates were used as curing agents. Polyisocyanates were

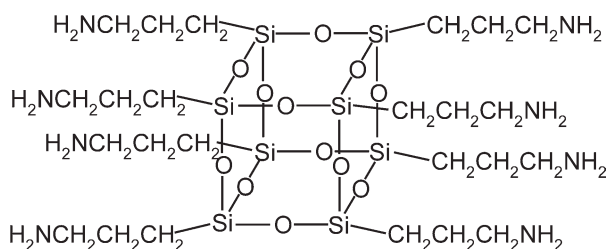


**Figure 1** The molecular structure of the octa(3-aminopropyl)octasilsesquioxane (POSS).

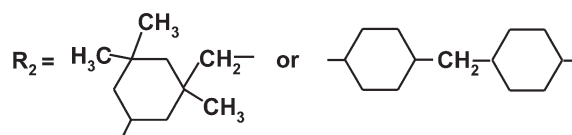
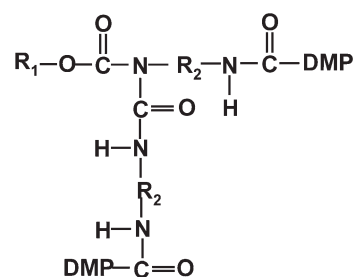


**Figure 2** The molecular structure of the internally-blocked polyisocyanate contained allophanate bonds.

synthesized according to the procedure as described in details in earlier reports.<sup>10,11</sup> The synthesis covered three stages: synthesis of urethane polyisocyanate, synthesis of allophanate, and blocking reaction.

Urethane polyisocyanates were obtained in the reaction of diisocyanate and alcohol at the molecular ratio of 2 : 1, in the presence of dibutyltin dilaurate as well as triethylamine as catalysts (both at 0.1 wt % with respect to diisocyanate), at the temperature of 60 ± 1°C. To synthesize allophanate linkages, the reaction mixture was heated up to 130 ± 1°C, stirred and refluxed for 5 up to 10 h, depending on the kind of urethane polyisocyanate. Free -NCO groups were subjected to blocking at the final stage. A calculated amount of the blocking agent was added to reaction mixture. The reactions were carried out in THF at the temperature of 60 ± 1°C. The products were evaporated under vacuum and dried at the temperature of 100 ± 1°C to remove the solvent. The obtained products were marked with symbols, e.g., IPDI-BU-DMP, where individual segments stand for the names of the feeds used. The molecular structure of internally-blocked polyisocyanate contained allophanate bonds were presented in Figure 2 and the characteristics of the obtained products were presented in Table I.

### Preparing lacquer compositions and coatings

The crosslinking agent was mixed with polyester resin Rucote 102 (NCO : OH molar ratio = 1 : 1). The samples IPDI-BU-RU102-POSS3% and IPDI-BU-RU102-POSS5%, which contained 3 and 5% POSS, were mixed at the molar ratio of NCO : OH and NH<sub>2</sub> = 1 : 1. The mixture was pulverized to the average particle size of 60 μm. The final powder coating was applied manually to steel and glass panels and cured

**TABLE I**  
**Specifications for the Obtained Powder Coatings**

Type of diisocyanate	Type of alcohol	Type of blocking agent	Symbol of polyisocyanate sample	Curing temperature (°C)	Curing time (min.)	Symbol of powder coating
IPDI	Methanol	DMP	IPDI-ME-DMP	180	40	IPDI-ME-RU102 <sup>a</sup>
IPDI	1-Butanol	DMP	IPDI-BU-DMP	180	40	IPDI-BU-RU102 <sup>a</sup>
IPDI	1-Hexanol	DMP	IPDI-HE-DMP	180	40	IPDI-HE-RU102 <sup>a</sup>
H <sub>12</sub> MDI	Methanol	DMP	H <sub>12</sub> MDI-ME-DMP	150	50	H <sub>12</sub> MDI-ME-RU102 <sup>a</sup>
H <sub>12</sub> MDI	1-Butanol	DMP	H <sub>12</sub> MDI-BU-DMP	150	50	H <sub>12</sub> MDI-BU-RU102 <sup>a</sup>
IPDI	1-Butanol	DMP	IPDI-BU-DMP	180	90	IPDI-BU-RU102-POSS3%
IPDI	1-Butanol	DMP	IPDI-BU-DMP	180	90	IPDI-BU-RU102-POSS5%

<sup>a</sup> The data were taken from the Refs. 10 and 11.

at 150–180°C for 40–90 min. The characteristics of so obtained lacquers were presented in Table I.

## Measurements

### Gloss

A micro-TRI-gloss tester from Byk Gardner was employed, according to the standard PN-EN ISO<sup>13</sup> for the angles of 20, 60, and 85°. The values specific for the coatings gloss were collected in Table II.

### Polarized optical microscopy

The surface of the powder lacquers were observed with the use of a Nikon ECLIPSE LV100 POL polarizing light optical microscope equipped with a polarizing filters, THMS-600 Linkam microscope hot stage and a Linkam TMS-94 temperature controller with liquid nitrogen cooling, used to provide the thermal control of the samples under the microscope within the temperature range of from 25 to 180°C. The temperature controller provided for the application of precise, programmable heating and cooling rates to the sample inside the microscope hot stage, as well as precise, programmable isothermal conditions ( $\pm 0.03^\circ\text{C}$ ). It may be used to study thermal-optical properties of the condensed phase, such as: phase transitions, crystalline structures in materials, anisotropy in materials, polymerization and degradation processes. A heating or cooling rate of  $10^\circ\text{C min}^{-1}$  was employed in all of the experiments. Isothermal deblocking and curing at 180°C was monitored over 20 min, until no more bubbles were evolved. All of the measurements were collected employing a  $5 \times$

microscope lens with a diameter 23.5 mm. Images were recorded an DS5Mc-L1 camera linked to computer via NIS – Elements Basic Research software.

### Surface topography and roughness measurements

The surface topography of the powder lacquers were investigated with the use of a Olympus Confocal Laser Scanning Microscope (CLSM) LEXT OLS3100 with capability an accurate three-dimensional measurement and sub-micron imaging, with outstanding 0.12  $\mu\text{m}$  resolution. The 408 nm laser diode combined with optics specifically enable magnification power from 120x to 14,400x.

The values of SR<sub>p</sub>, SR<sub>v</sub>, SR<sub>z</sub>, SR<sub>c</sub>, SR<sub>a</sub>, SR<sub>q</sub> and SR<sub>zjis</sub> were used to characterize the coating roughness parameter. These were calculated according to the following formulas:

SR<sub>p</sub> – max. peak height (Z<sub>p</sub>) of roughness curved surface,

SR<sub>v</sub> – max. valley depth (Z<sub>v</sub>) of roughness curved surface,

SR<sub>z</sub> – max. height roughness. Sum of max. peak height (Z<sub>p</sub>) and max. valley depth (Z<sub>v</sub>) in contour curved surface

SR<sub>c</sub> – mean peak height of roughness curved surface,

SR<sub>a</sub> – arithmetic mean roughness. Mean absolute value of  $f(x,y)$  in contour curved surface:

$$\text{SR}_a = \frac{1}{LM} \int_0^M \int_0^L |f(x,y)| dx dy$$

SR<sub>q</sub> – root mean square roughness,

**TABLE II**  
**Specifications of the Coatings Roughness and Gloss**

Symbol of powder coating	SR <sub>p</sub>	SR <sub>v</sub>	SR <sub>z</sub>	SR <sub>c</sub>	SR <sub>a</sub>	SR <sub>q</sub>	SR <sub>zjis</sub>	Gloss 20°/65°/80° (%)
IPDI-BU-RU102	0.662	0.171	0.834	0.106	0.063	0.091	0.767	25/61/55 <sup>a</sup>
IPDI-BU-RU102-POSS5%	5.633	1.007	6.640	1.403	0.472	0.644	6.561	6/28/30

<sup>a</sup> The data were taken from the Ref. 11.

**TABLE III**  
The Surface Free Energy Values and Their Components for Model Liquids

Model liquid	$\gamma_L$ [mJ/m <sup>2</sup> ]	$\gamma_L^{LW}$ [mJ/m <sup>2</sup> ]	$\gamma_L^{AB}$ [mJ/m <sup>2</sup> ]	$\gamma_L^+$ [mJ/m <sup>2</sup> ]	$\gamma_L^-$ [mJ/m <sup>2</sup> ]
Water	72.8	21.8	51	25.5	25.5
Formamide	58.0	39.0	19	2.28	39.6
Diiodomethane	50.8	50.8	0	0	0

$$SRq = \sqrt{\frac{1}{LM} \int_0^M \int_0^L f(x, y)^2 dx dy}$$

where: *L*-length in *X*-direction of contour curved surface, *M*- that in *Y*-direction of contour curved surface, and profile curved surface  $y = f(x, y)$ .

SRzjis – 10-point mean roughness. Sum of the mean height of the highest five peaks of roughness curve and the mean depth of the deepest five valleys:

$$SRzjis = \frac{1}{5} \sum_{j=1}^5 (Zpj + Zvj)$$

The values specific for the coatings roughness were collected in Table II.

Determination of surface free energy (SFE)

Surface free energy ( $\gamma_s$ ), is quantified using a contact angle goniometer made by Cobrabid-Optic. As immersed liquids diiodomethane, formamide and water were chosen. Measurements were realized at  $22 \pm 1^\circ\text{C}$ . The surface free energy values and their components for model liquids were collected in Table III.

Contact angles those three liquids with known values of  $\gamma_L$ ,  $\gamma_L^{LW}$ ,  $\gamma_L^+$  and  $\gamma_L^-$  (Table III) are put into the following equation (acid-base model by van Oss)<sup>14</sup>:

$$(\gamma_S^{LW} \gamma_{Li}^{LW})^{0.5} + (\gamma_S^+ \gamma_{Li}^-)^{0.5} + (\gamma_S^- \gamma_{Li}^+)^{0.5} = \gamma_{Li}(1 + \cos \Theta_i)/2$$

where  $\gamma$  refers to surface free energy, the subscripts *Li* and *S* refer to liquid and solid, and the super-

scripts *LW*, *+* and *-* refers to dispersive, acid and base components. The total surface free energy of the solid is then given by:

$$\gamma_s = \gamma_s^{LW} + \gamma_s^{AB} = \gamma_s^{LW} + 2(\gamma_s^+ \gamma_s^-)^{0.5}$$

Calculations based on these measurements produce a parameter (critical surface tension or surface free energy), which quantifies the characteristics of the solid and mediates the properties of the solid substrate.

The surface free energy values and their components as calculated from the measurements of wetting angles for powder coatings were collected in Table IV.

**RESULTS AND DISCUSSION**

Blocked polyisocyanates synthesized as described in earlier reports were used as curing agents for investigated powder lacquer coatings.<sup>10,11</sup> Those polyisocyanates were synthesized from cycloaliphatic diisocyanates IPDI and H<sub>12</sub>MDI, and from monohydric alcohols: methanol, ethanol, 2-propanol, 1-butanol, and 1-hexanol. The crosslinking agents with allophanate linkages in their structures made it possible to minimize the required amount of a blocking agent. That, in turn, reduced the volume of volatile organic compounds (VOC), which were released from the hardening process.<sup>15</sup> The commercial polyester resin Rucote 102 from Bayer made the principal component of the lacquer. The lacquer blends were prepared with the use of additives which improved leveling (Resiflow PV 88) and eliminated gas bubbles (WorleeAdd 902) in the hardening operation. To modify the surface properties, octa(3-aminopropyl)octasilsesquioxane was introduced

**TABLE IV**  
Compilation of Surface Free Energy Values and Their Components as Calculated from the Measurements of Wetting Angles

Symbol of powder coating (as per Table I)	Surface free energy values and their components [mJ/m <sup>2</sup> ]				
	$\gamma_S^{LW}$	$\gamma_S^+$	$\gamma_S^-$	$\gamma_S^{AB}$	$\gamma_s$
ME-IPDI-RU102	40,65	$4.46 \times 10^{-3}$	9.10	0.40	<b>41.06</b>
BU-IPDI-RU102	40,83	$1.36 \times 10^{-5}$	8.64	0.02	<b>40.85</b>
HE-IPDI-RU102	40,79	$9.0 \times 10^{-5}$	8.57	0.05	<b>40.85</b>
ME-H <sub>12</sub> MDI-RU102	41,73	$1.61 \times 10^{-3}$	9.38	0.24	<b>41.97</b>
BU-H <sub>12</sub> MDI-RU102	40,74	$8.16 \times 10^{-3}$	7.26	0.49	<b>40.96</b>
BU-IPDI-RU102-POSS5%	42,39	0.104	5.33	1.49	<b>43.88</b>



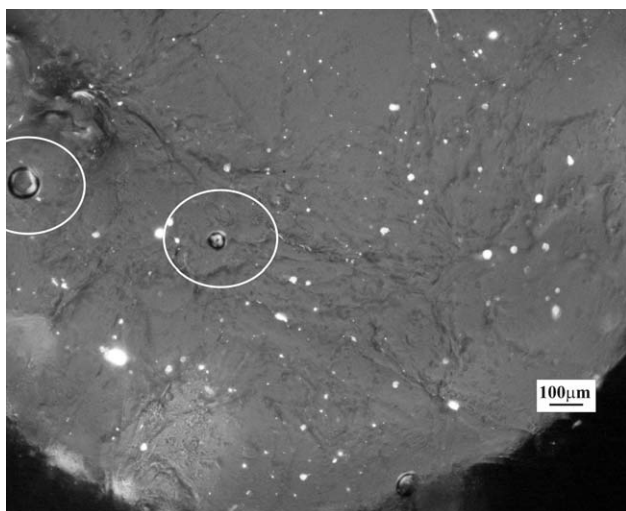


**Figure 3** The optical image of the powder composition IPDI-BU-RU102-POSS5% at 122°C. The bubbles of the released blocking agent were visible.

(3 and 5%) at the lacquer blending stage. Amine groups in octa(3-aminopropyl)octasilsesquioxane reacted under hardening conditions with isocyanate groups of polyisocyanate to yield urea bonds. Unmodified samples and those modified with POSS were used in surface visualization and in studies on the hardening process.

#### Visualization of the coating formation process with the use of a polarized optical microscope

In powder coatings, an understanding of the process by which a deposited powder is converted to a cured film requires the investigation of several properties. Namely surface characteristics, surface tension and cure behavior. The surface properties can be correlated with the chemical structures of resin and curing agent, processing condition and other formulation properties of the powder system, allowing control of surface appearance. In this section, the cure behavior of the coatings in the heating-cooling cycle was examined with a POM, in the reflected light. To this end, the powder lacquer composition was applied to the microscopic slide and placed on the stage of the microscope provided with a heating unit.

The optical image of the powder composition at 25°C demonstrated powder grains representing individual lacquer components. However, it was impossible to distinguish from the obtained image which grains represented which components. Similar images were also obtained for blends with different compositions. The blend melting process began at 88°C, and it was most intense at 96–98°C. The first bubbles appeared at 120°C – they came from the released blocking agent, i.e. 3,5-dimethylpyrazole (Fig. 3). The number of gas bubbles increased at further heat-up. To evaluate the time for deblocking, the sample was

observed at isothermal conditions, at 180°C. In case of samples which contained no POSS, the observed bubbles gradually reduced their volume or burst, and they finally disappeared after about 20 min. The samples modified with POSS, because of the possible reaction between POSS and polyisocyanate, contained an adequately higher amount of the crosslinking agent. More bubbles were formed in that case and the deblocking process took much longer to completion (up to about 40 minutes). The deblocking process was assumed to come to an end when no more bubbles were released. The hardening process of the lacquer coating was also initiated at that moment. Some small movements were observed within the coating composition, but the composition gradually stabilized after formation of gas bubbles ceased, and finally the image became invariable (Fig. 4). The sample was cooled down then. During that phase, as early as at 140°C, first light-yellow colored spots were observed which were indicative for the beginning of the microseparation and crystallization process. The rigid segments within the PU chains which were formed in the crosslinking process, composed of urethane bonds, ester bonds, and aromatic rings (derived from isophthalic acid), undergo microseparation from flexible segments and the hard phase is produced in this way. Hydrogen bonds are formed between urethane groups and ester groups which are components of said hard phase; and that provides additional and favorable conditions for crystallization. The size of those spots increased when the sample temperature was going down (Fig. 5). That suggests further advancements in the microseparation process. Crystallization of separated phases was initiated below 25°C. The higher the microseparation level, the higher the ability to crystallize is.<sup>16</sup> The crystallization process reached its end after about 1 h (Fig. 6). The picture shows clearly the crystalline structures, which underwent no changes after 1 week. The crystalline

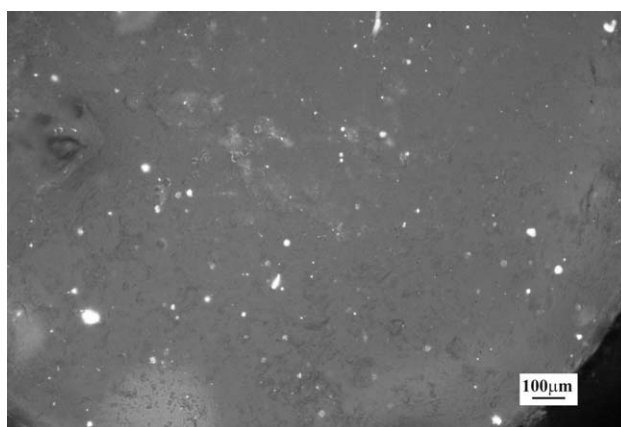


**Figure 4** The optical image illustrates the hardening process of the powder composition IPDI-BU-RU102-POSS5% observed at isothermal conditions at 180°C after 40 min.

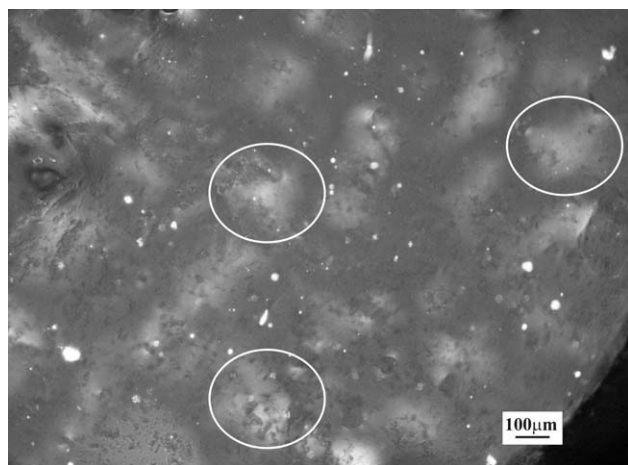


**Figure 5** The optical image of the powder coating IPDI-BU-RU102-POSS5% when the temperature was going down to 40°C. The light-yellow colored spots were observed.

structures, which were formed in the samples with no POSS, were much bigger (Fig. 7).

The presence of a large size molecule of octa(3-aminopropyl)octasilsesquioxane (POSS) which is incorporated in the PU structure through eight urea groups pushes the polyurethane chains aside. That reduces the tendency to create hydrogen bonds which makes a considerable impediment for the crystallization process.

#### Presentation of three-dimensional surface topography by confocal scanning laser microscopy

Using this technique, the three-dimensional powder composition and surface topographies of the thermosetting powder coatings were obtained. This method is well-suited to the investigation of surface struc-

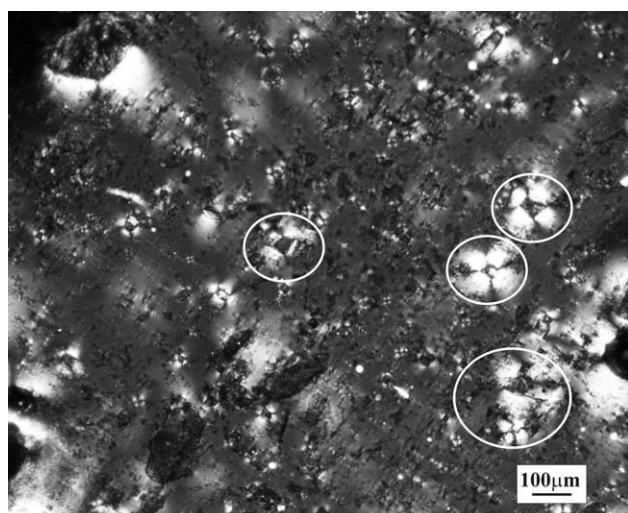


**Figure 6** The optical image of crystalline structures of the powder coating IPDI-BU-RU102-POSS5% after 30 min when the temperature was going down to 25°C.

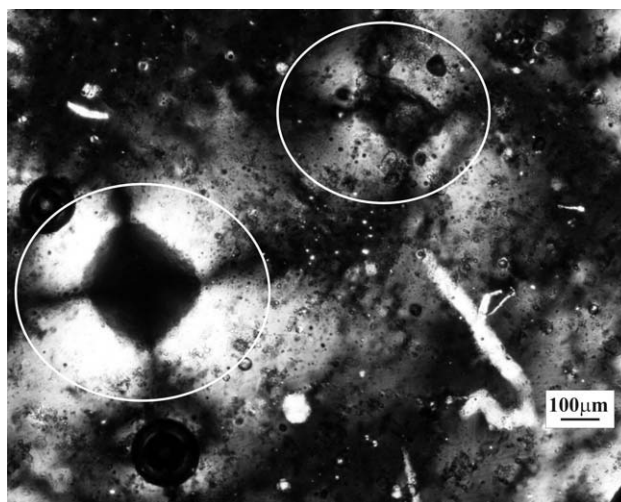


**Figure 7** The optical image of crystalline structures of the powder coating IPDI-BU-RU102 after 30 min when the temperature was going down to 25°C.

tures. The confocal laser scanning microscope image for powder composition was shown in Figure 8.

The shape of the grains formed is clearly diversified, depending on the direction considered. There are no essential differences in the grain surface along axes X and Y, while distinct irregularity is observed along the perpendicular direction (i.e. along axis Z). The maximum valley depth on the grain surface amounts to  $SR_v = 36 \mu\text{m}$ . The grain size along axis X is about 70  $\mu\text{m}$ , along axis Y – about 60  $\mu\text{m}$ , and the grain height, i.e. the size along axis Z, reaches 56  $\mu\text{m}$ . That technique is not applicable in distinguishing definitely which grain is formed by which component present in the lacquer coating formulation.

The three-dimensional topographies of powder coating IPDI-BU-RU102 was shown in Figure 9. The surface was smooth. The surface of the POSS contained powder coating exhibits much larger

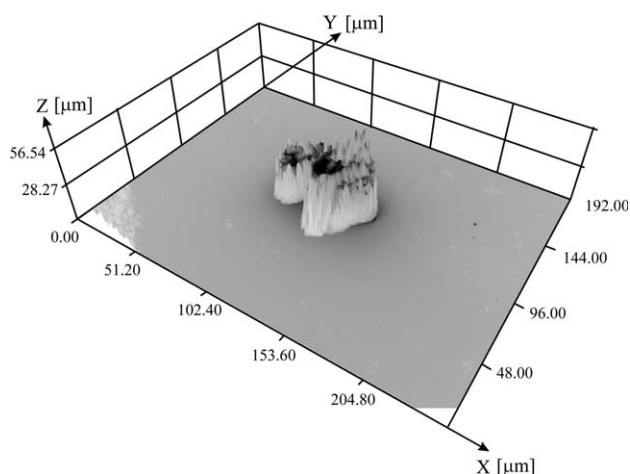


**Figure 8** The confocal laser scanning microscope image of powder composition IPDI-BU-RU102.



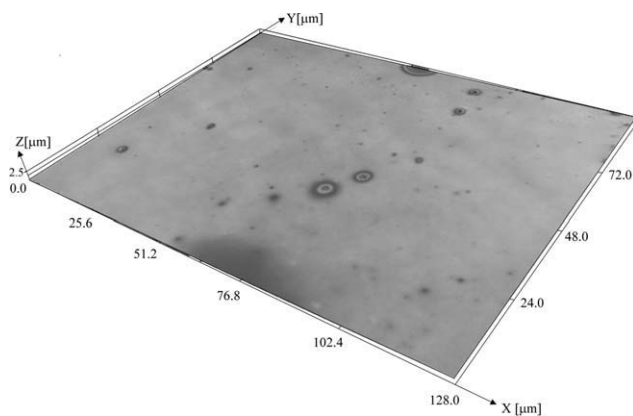


**Figure 9** The confocal laser scanning microscope image of powder coating IPDI-BU-RU102.

irregularity and roughness (Fig. 10). The values for surface roughness ( $SR_p$ ,  $SR_v$ ,  $SR_z$ ,  $SR_c$ ,  $SR_a$ ,  $SR_q$ , and  $SR_{zjis}$ ) are higher in this case than those for the IPDI-BU-RU102 system (Table II).

### Gloss

The values of the specular gloss, measured for the IPDI-BU-RU102 coating at the angles of 20, 65, and 80°, were 25, 61, and 55%, respectively (Table II). Those values were higher than those for the POSS-containing samples (6, 28, and 30%). The surface appearance of the IPDI-BU-RU102 coating was semi-gloss (the values measured for the gloss were in the range 45–70% for the angle of 65°), while the surface of IPDI-BU-RU102-POSS5% was semi matt (the values measured for the gloss were in the range 25–45% for the angle of 65°).

The gloss of the coating was strongly affected by the surface roughness and irregularity. The superficial structure, however, is closely determined by the chemical structure of the coating. The higher the

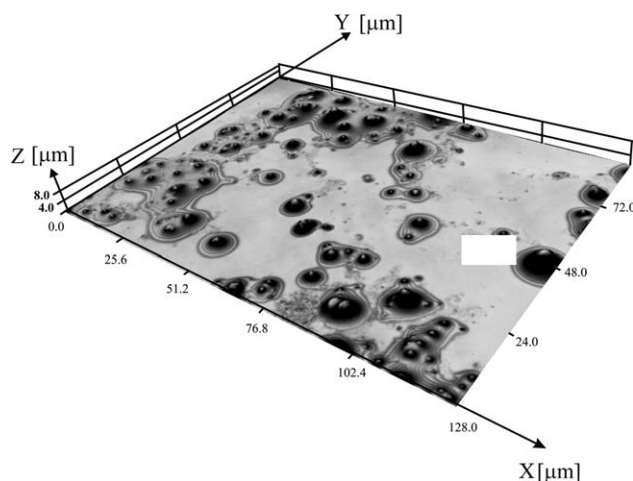


**Figure 10** The confocal laser scanning microscope image of powder coating IPDI-BU-RU102-POSS5%.

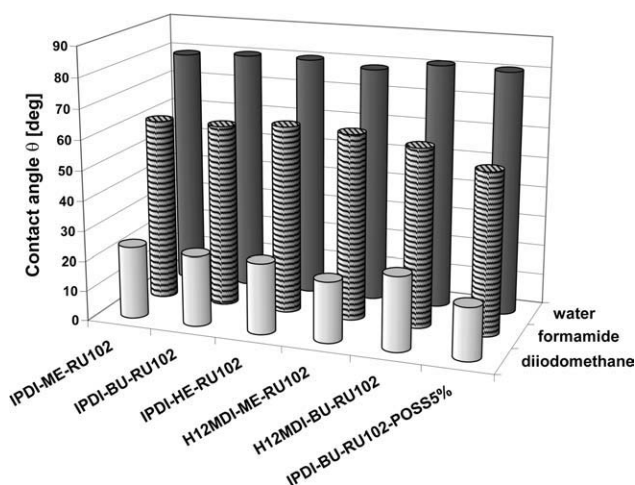


**Figure 11** Comparison values of wetting angles for the studied coatings measured for three model liquids: water, formamide and diiodomethane.

gloss, the better micro-homogeneity of the coating. The presence of urethane bonds, biuret bonds, and allophanate bonds, added to urethane bonds and other heteroatoms, contribute to extended micro-inhomogeneity of the system, which is observed as a reduction in gloss. The discussed escalation in superficial micro-inhomogeneity of the samples which contained POSS resulted from the presence of silicon atoms and high amounts of urea bonds which were formed in the reaction of eight groups  $-NH_2$  in POSS with polyisocyanate.

### Surface free energy

To find the values of surface free energy (SFE), wetting angles were measured for three model liquids: water, formamide, and diiodomethane (Table IV). Figure 11 puts together the measured values of wetting angles for the studied coatings. Water and formamide (bipolar liquids) form big drops on the coating surface (within 53 to 81°), while much lower wetting angle values are specific for diiodomethane (nonpolar liquid), from 17 to 25°. As results from the data given in Table III, the surface free energy values for the studied polyurethane coatings fall within the range of 40.85–43.88  $\text{mJ}/\text{m}^2$ . Those values classify the studied coatings as medium-polarity ones. The obtained data suggest that a major contribution to the total surface energy is made by the “amount” of dispersion interactions, which is quantitatively expressed by the parameter  $\gamma_s^{LW}$ , and which is dependent on the structure of macromolecules. Acid–base interactions control the SFE value to a small degree only. The quantitative contribution from  $\gamma_s^{AB}$  never exceeds 0.5%. The SFE values for the coatings which have not been modified with POSS differ from each other slightly only. Thus, no

unequivocal conclusions may be drawn on the structural effects from crosslinking agents on SFE. Most probably, the decisive effect on the SFE value comes from the polyester resin material which constitutes nearly 90% in all compositions. The SFE value for the POSS-containing coatings is slightly higher than for other coatings. A high-volume POSS molecule, which contains polar groups, when incorporated into the polymer chain, added to the polar nature of the coating which increased its SFE value. The acid-base component  $\gamma_S^{AB}$  is also highest for that type of coating, which results from the alkaline nature of POSS.

### CONCLUSIONS

The modern optical microscopy with programmable sample heating was employed to observe: powder formulation melting process, polyisocyanate deblocking process, formation of lacquer coating, and supermolecular structures which were formed when the sample temperature was going down. It was also possible to determine temperature and time parameters for melting, deblocking, and crosslinking of the lacquer coat. Those parameters are useful when the coat blending conditions are defined, e.g. when the proper extrusion temperature is selected, and also when the lacquer stoving temperature and time are optimized. The confocal microscopy made the 3-D visualization of the lacquer surfaces possible, and it enabled calculation of the surface roughness parameters. It should be noted that both the methods presented in this paper are sufficiently general to be applicable in studying other polymer materials as well.

The obtained results were referred to gloss, surface free energy, and chemical structure of the coats.

The obtained data reveal unequivocally that both gloss and surface free energy were closely related to the superficial structure, which in turn is determined by the chemical structure. The more homogeneous the coat was from the viewpoint of its chemical structure, the bigger its crystallites and the highest the surface quality and gloss were.

The authors would like to thank Olympus Poland for taking confocal laser scanning microscope images, as well as Bayer A.G., Evonik Degussa G.m.b.H. and Worlée-Chemie G.m.b.H for sending free samples of raw materials.

### References

1. Chattopadhyay, D. K.; Raju, K. V. S. N. *Prog Polym Sci* 2007, 32, 352.
2. Kozakiewicz, J.; Kuczyńska, H. *Ochrona przed korozją* 2008, 12, 440.
3. Wang, J.; Wang, L. *J Fluor Chem* 2006, 127, 287.
4. Yang, J.; Zhou, B.; You, B.; Wu, L. *JCT Res* 2006, 3, 333.
5. Chen, X.; You, B.; Zhou, S.; Wu, L. *Surf Interface Anal* 2003, 35, 369.
6. Lee, S. S.; Han, H. Z. Y.; Hilborn, J. G. *Prog Org Coat* 1999, 36, 79.
7. Majumdar, P.; Webster, D. C. *Polymer* 2007, 48, 7499.
8. Turri, S.; Radice, S.; Canteri, R.; Speranza, G.; Anderle, M. *Surf Interface Anal* 2000, 29, 873.
9. Wu, W.; Zhu, Q.; Qing, F.; Han, C. *Langmuir* 2009, 25, 17.
10. Pilch-Pitera, B. *Przem Chem* 2009, 8, 892.
11. Pilch-Pitera, B. *J Appl Polym Sci* 2010, 116, 3613.
12. Choi, J.; Yee, A. F.; Laine, R. M. *Macromol* 2003, 36, 5666.
13. Determination of specular gloss of non-metallic paint films at 20°, 60° and 85°, PN-EN ISO 2813, Polish Committee for Standardization, Paints and varnishes, Warsaw, Poland, 2001.
14. Żenkiewicz, M. *Adhezja i modyfikowanie warstwy wierzchniej tworzyw wielkocząsteczkowych*; WNT: Warsaw, 2000;
15. Rawlins, J. W.; Feng, R.; Sullivan, C.; Thometzek, P. *Paint Coat Ind* 2002, 18, 38.
16. Król, P.; Pilch-Pitera, B. *J Appl Polym Sci* 2007, 104, 1464.